scientific reports



OPEN

Multilayer patch functionalized microfibrillated cellulosic paper sensor for sweat glucose monitoring

Zoheb Karim^{1™}, Mohd Jahir Khan², Afzal Hussain³, Faheem Ahmed⁴ & Zishan Husain Khan⁴

Electrochemical analysis of glucose monitoring without painful blood collection provides a new noninvasive route for monitoring glucose levels. Thus, in this study, biobased cellulosic papers (methylated and phosphorylated one) based glucose monitoring sensor is developed. To achieve high hydrophilicity, microfibrillated cellulose (MFC) were functionalized using hexokinase mediated phosphorylation (–OH to –S O_3^{2-}). The instinctive increased surface charge density from 36.2 \pm 3.4 to 118.4 ± 1.2 µmol/q and decrease contact angle (45°-22°) confirms the increased hydrophilicity of paper. Furthermore, functionalized phos-MFC paper increase the capillary flow of sweat, required low quantity (1 µl) of sweat for accurate analysis of glucose level. Additionally, chemically induced methyl groups (-CH₂) make the sensor more barrier to other chemicals. In addition, a multilayer patch design combined with sensor miniaturization was used to lead to an increase in the efficiency of the sweat collection and sensing processes. Besides, this paper sensor integrated with artificial transdermal drug delivery unit (agarose gel as skin) for monitoring glucose levels in sweat. The patch monitoring system increase the accuracy of sensing with fluctuation in sweat vol. (1–4 μl), temperature (20–70 °C), and pH (4.0-7.0). In addition, temperature dependency artificial transdermal delivery (within agarose gel) of drug metformin agrees the measurement accuracy of sensor, called "switch system" without any error. As a result, the reported MFC paper based multi-patch disposable sensing system provides a novel closed-loop solution for the noninvasive sweat-based management of diabetes mellitus.

Keywords Glucose, Sweat, Sensor, Functionalized MFC paper, Multilayer patch sensing, Phosphorylated MFC, Methylated MFC

Abbreviations

MFC Microfibrillated cellulose
WHO World Health Organization
polyPEDOT Poly(3-4-ethylenedioxythiophene)

GOx Glucose oxidase

PBS Phosphate buffered saline BSA Bovine serum albumin

PANi Polyaniline

PDMS Polydimethylsiloxane
PCNs Phase change nanoparticles
PCM Phase change materials
SEM Scanning electron microscopy

DMS Dimethyl sulfide PI Polyimide

¹MoRe Research Örnsköldsvik AB, SE-891 22 Örnsköldsvik, Sweden. ²Department of Chemical Engineering, Faculty of Engineering, Mahidol University, Nakhon Pathom 73170, Thailand. ³Department of Pharmacognosy, College of Phamacy, King Saud University, PO Box 2457, 11451 Riyadh, Saudi Arabia. ⁴Department of Applied Sciences and Humanities, Faculty of Engineering and Technology, Jamia Milia Islamia, New Delhi 110025, India. [™]email: zoheb.karim@qmail.com

Glucose is one of the most globally important and clinically investigated biological compounds. The extensive interest in this analyte is related to diabetes, a metabolic and chronic disease that causes abnormal levels of glucose in the blood^{1–5}. According to the World Health Organization (WHO), the number of people who live with diabetes almost quadrupled over the last 24 years. It is estimated that about 8.5% of the world's population has been diagnosed with diabetes⁶. Diabetes is tightly linked with uncontrolled blood sugar levels, which lead to many complications and damage to vital organs. While in developed countries, screening blood for irregularities is typically performed as part of a routine checkup, measurements of blood glucose are accessible only in the 50% of the primary care settings in low-income countries^{7–9}.

With the evolution of microelectronics and possibility of automation, electrochemical sensors have come to the forefront of real-world clinical applicability by demonstrating reliable performance in detecting glucose levels^{10–12}. The majority of current electrochemical metabolite sensors rely on the function of enzymes, namely, oxidoreductases mounted on hard supports^{13,14}; indeed, fabrication of traditional "hard" electronics typically involves tedious and expensive processing methods due to the nature of the electrode materials. In addition to the low frequency rate of monitoring, using a whole-blood sample introduces complications, first in terms of the pain and inconvenience that multiple needle pricks cause and second in terms of the requirement for trained personnel who perform such tests in some cases. Therefore, self-monitoring of critical biomarkers in the body using biofluids alternative to blood, such as saliva^{15,16} and sweat^{17–19}, is in high demand. Consequently, extensive efforts have been made to develop flexible noninvasive sweat-based biomarker monitoring methods. Wearable flexible biosensors enable continuous monitoring of metabolites, including glucose^{20–23}, lactate²⁴, and alcohol²⁵.

In this study, a flexible strip-type paper-based device was designed for monitoring glucose in sweat using a noninvasive approach. Till our information, it's a first study introduced the integrated concept of functionalization of commercial microfibrillated cellulose (MFC) and electrode printing. Commercially available MFC was functionalized and then vacuum filtered to fabricate paper for printing electrodes.

Indeed, our group is working immensely close to surface functionalization of cellulose for flexible paper production. Various surface functional groups (SO_3^{2-} , PO_4^{2-} , CH_3 , -COO, -OH)^{26–28} were introduced on/ in MFC using enzymatic and chemical catalysis. To test the impact of functionalization, charge density of introduced functional groups was calculated and the flexibility of produced paper was measured using tensile modules. Furthermore, fabricated cellulosic paper was applied for various applications like pollutants separation, flexible composite membranes and protein purification^{26,27}. Indeed, in this study, an enzymatic and chemical functionalized flexible cellulosic paper has been used for printing of multilayer patch sensing system. Additionally, to increase the capillary adsorption of sweat, MFC was functionally modified using enzyme hexokinase, introduced phosphate groups (PO_4^{2-}) make the cellulosic paper highly hydrophilic, certainly, increase the adsorption of sweat for accurate measurement. In another functionalization route, a chemical induced methylation was performed to make the cellulosic paper more hydrophobic. The increase hydrophobicity of cellulosic paper increases the barrier property of used printed paper.

Furthermore, in our opinion, an improved design of a paper-based sensor called" multilayer patch system" has been introduced, where accuracy of a sensing could be increase by assembling three sensing devices together. We have hypothesized that the green functionalization (enzyme hexokinase-based surface modification) of cellulosic paper would induced the capillary adsorption of sweat for accurate sensing of glucose. Additionally, this noninvasive route for monitoring patients with multilayer patch system could be the breakthrough in pharmaceutical science respect to amount of sweat needed for measurement, indeed, only 1 µl sweat was used glucose measurement. Additionally, this study also introduces the controlled release of drug for diabetes mellitus. Besides, several other key advantages of such system can be; (1) paper-based flexible disposal system, (2) scalable capability (production compatibility) production of electrodes, (3) miniaturized design with high accuracy glucose monitoring, (4) disposable design for enhancing practical applicability, (5) multiple sweat control and uptake layers for monitoring sweat collection, (6) detection of small amounts of glucose in sweat with high sensitivity, and (7) multistage and controlled transdermal drug delivery *via* biocompatible polymeric microneedles.

Likewise, in this study, metformin was used as first line drug for treating type-2 diabetes²⁹. Because drug delivery through the skin bypasses the digestive system, transdermal delivery of metformin requires a lower dose of drug than that in oral delivery, which also prevents metformin-induced gastrointestinal side effects³⁰. This novel system for high-fidelity sweat glucose measurement and feedback-controlled drug delivery enables efficient management of blood glucose concentration without pain and stress. To test the drug delivery an artificial agarose gel system (corresponds to human skin) was used for the study and the hardness of agarose gel was maintained close to skin.

Experimental Functionalization of MFC

The methylation of MFC was performed as reported in our previous article²⁸, in detail, MFC (1 wt%) was mercerized using 60 ml NaOH solution (50% m/v) for 1 h at room temperature. The excess NaOH was removed by filtration and acetone (27.0 ml) was added as a solvent. Dimethyl sulfide (DMS) (9.0 mL) was added dropwise, and the reaction was carried out at 50 °C. After 1 h of reaction, the system was filtered and fresh reagents were added (acetone and DMS), maintaining the same previous proportions. At the end, the sample was neutralized using acetic acid (10% v/v), filtered, and washed with acetone (three times with 90 ml) and finally dried in an oven at 50 °C for 6 h.

Furthermore, green phosphorylation of MFC (1 wt%) using enzyme hexokinase was performed previously. Briefly, reaction proceeds in 1 wt% of MFC in phosphate buffer (pH 7.6) in the presence of a 50 mM ATP, 50, 100 and 200 mM of MgCl, and 35 U ml $^{-1}$ of enzyme for 24 h at 30 $^{\circ}$ C $^{31-33}$.

Fabrication and characterization of MFC papers

The 0.5 wt% MFC (phosphate-MFC and methylated-MFC) was filtered through vacuum-filtration device (600 ml capacity). Obtained filter cake was dried for 48 h and approx. 2 kg pressure was applied for wrinkle free paper production. The paper was stored at room temperature for further use³¹.

Furthermore, the concentration of phosphate groups on MFC was determined using Inductive Coupled Plasma Atomic Emission Spectroscopy (ICPOES, Optima 2000 DV, Perkin Elmer, USA) after the mineralization of native and phosphorylated-CMF samples in boiling HNO_3 and H_2O_2 . To ensure the acidic form of phosphate groups, samples were first washed several times with diluted HCL to pH 4.0 and then mineralized³⁴.

The determination of methyl groups content was made through the method discussed by Chen³⁵ with some modifications as discussed by Viera et al.³⁶.

The tensile strength of both produced papers including pristine-MFC paper was measured using a tensile tester (Lorentzen &Wettre, ABB, Sweden), as discussed in our recently published article³⁷.

Air permeance of samples was measured using L&W air permeance tester (Lorentzen &Wettre, ABB, Sweden). First, calibration of the tester was performed, and then samples were placed under holder and defined air pressure was applied.²⁸.

Device array fabrication

Spin coating of the polyimide (PI) precursor (1.5 μ m; Sigma-Aldrich, USA) on an SiO₂ plate followed by thermal curing of PI was performed. A thin film of Cr/Au (\approx 40 nm/ \approx 100 nm) was deposited by thermal evaporation on the electrodes. Additionally, a Cr/Pt film (\approx 20 nm/ \approx 120 nm) was deposited by sputtering and patterned using photolithography for the temperature sensor and the counter electrode of the glucose sensor. The top epoxy layer (\approx 2 nm) was coated and then patterned using a combination of photolithography and reactive ion etching. The device was transfer-printed onto a cellulosic substrate using water-soluble tape. The strip-type device was then constructed on the film using the same procedure.

Functionalization via electrochemically active materials

For electrodeposition of poly(3-4-ethylenedioxythiophene), polyPEDOT, a solution of 0.01 M 3,4-ethylenedioxythiophene (Sigma-Aldrich) and 0.1 M LiClO $_4$ (Sigma-Aldrich) in acetonitrile was prepared. The electrode was dipped in the solution, and galvanostatic electrodeposition was performed for 30 s at 1.3 V (potential versus commercial Ag/AgCl electrode).

Ag/AgCl electrodeposition was performed in an aqueous solution (5 mM) AgNO $_3$ into which the electrode was dipped. The potential ranged from -0.9 to 0.9 V versus an Ag electrode for 14 segments at a scan rate of 0.1 Vs $^{-1}$. The electrode was then dipped in 0.1 M each of KCl and HCl to chlorinate it after which the potential was swept from -0.15 to 1.05 V versus a commercial Ag/AgCl electrode for four segments at a scan rate of 0.05 Vs $^{-1}$.

An aqueous solution of 2 mM HAuCl₄ in 2 M H_2SO_4 was prepared for gold electrodeposition. The gold electrode was dipped into the prepared solution and electrodeposited using a galvanostatic method for 5 min at -1 V with a Pt counter electrode and a commercial Ag/AgCl electrode.

Prussian blue electrodeposition was performed in 10 mM KCl, 2.5 mM K $_3$ [Fe(CN) $_6$], and 2.5 mM FeCl $_3.6$ H $_2$ O in 0.1 M HCl mixture solution. The potential was swept from 0 to 0.5 V versus a commercial Ag/AgCl for two segments at a scan rate of 0.02 V s $^{-1}$.

Glucose oxidase (GOx) was immobilized for catalysis based on a detailed procedure. A chitosan solution (1wt%) in 2wt% acetic acid was prepared. The chitosan solution was mixed with an exfoliated graphite solution (2 mg/ml) in 1x phosphate buffered saline (PBS). The exfoliation process was performed using an ultrasonic machine (Sonics VCX-750, Vibra Cell) for 30 min. The chitosan/graphene solution was mixed with a GOx (0.05 m ml $^{-1}$) and 0.01 g/ml bovine serum albumin (BSA) mixture. A solution of GOx was also prepared in 1x PBS. The GOx and BSA (0.8 μ l) mixture in the PBS solution was drop cast on the gold-deposited electrode. After drying the electrode under ambient conditions, 0.8 μ l of GOx in the chitosan/grapheme solution was drop-cast on the electrode. After drying the electrodes under ambient conditions, 2 μ l of 0.5 wt% Nafion was drop cast on the glucose sensor. After drying the Nafion membrane in ambient air, 0.8 μ l of 2wt% glutaraldehyde was drop casted on the glucose sensor to ensure robust cross-linking of the enzyme layer 31 . the sweat was collected after cycling in Eppendorf and then printed sensor was dipped into the sweat for monitoring glucose.

Polyaniline (PANi) electrodeposition was performed in a solution of 0.1 M aniline (in 1 M HCl). The electrode was dipped into the solution, and the potential was swept from -0.2 to 1.0 V versus a commercial Ag/AgCl electrode for 60 segments at a scan rate of 0.1 Vs⁻¹.

Fabrication of microneedles

A polydimethylsiloxane (PDMS) mold was prepared using commercial microneedles. The microneedles had the height of 1 mm and a round base diameter of 250 µm. The drug-loaded (metformin) phase change nano particles (PCNs) combined with 2% hyaluronic acid were drop cast onto the mold. The sample was placed under vacuum until bubble generation had ceased. After degassing, the sample was dried at room temperature, and the microneedles were carefully peeled from the mold. The phase change material (PCM), tetradecanol, was sprayed on the microneedles, and a micro/nano morphological analysis was performed using Scanning Electron Microscopy (SEM).

All the studies performed in this article were free from animal and human contact, an artificial skin of agarose gel was developed to test the penetration of microneedles and delivery of metformin, furthermore, the sweat was collected from the human first and then tested in laboratory, no direct contact was made with human skin.

Fig. 1. The flow of studies in this article are shown in this image. High grade MFC (Exilva P 01-V) was purchased from Borregaard AB and further functionalized using enzyme-based phosphorylation and chemical modification for introduction of PO_4^{2-} and $-CH_3$ functional groups, respectively. Later printable paper was fabricated using vacuum-filtration. Multilayer patch sensor was printed on filtered MFC paper and then used for the measurement of glucose in sweat. The sweat was collected first and then measured in the laboratory, no direct contact of device with human skin was made

				Tensile strength (MPa)		
Hybrid membranes	Surface charge density (µmol/g)	Density (kg/m³)	Types of functional groups	Dry	Wet	Air permeance (μm/Pa, s)
Pristine-MFC	36.2 ± 3.4	220	-ОН	21.5 ± 2.3	6.7 ± 1.4	25
Methyl-MFC	7.9 ± 1.7	189	-CH ₃	15.1 ± 3.6	12.4 ± 1.3	16
Phosphate-MFC	118.4±1.2	200	$-PO_4^{2-}$	25.5 ± 1.3	4.1 ± 2.5	18

Table 1. Physical properties of produced sensor printing paper

Results and discussions Characterization of functionalized paper

In the article, functionalized MFC paper was used for the printing of sensor. The activities flow of the article is mentioned in Fig. 1. Two approaches were used for the functionalization of MFC, an enzymatic phosphorylation of Exilva P 01-V (MFC) was performed by enzyme hexokinase and in another approach chemical methylation o was performed as mentioned in Fig. 1. ALL characterization of functionalized paper is mentioned in Table 1.

The decrease surface charge density of vacuum filtered paper (methyl-MFC) from 36.2 ± 3.4 to 7.9 ± 1.7 µmol/g after methylation confirms the increase hydrophobicity of produced paper, which is further confirmed by increase in surface contact angle from 45 to 110° (Supplementary file, Figure S1). Furthermore, densification of methyl-MFC can also be seen by decrease in density and air permeance compared to pristine-MFC paper (Table 1). Separately, hexokinase mediated phosphorylation of MFC increases the surface charge density of introduced phosphate groups which has decrease in contact angle (45 to 25°) indicate high hydrophilic nature of filtered paper. The data is further supported by introduced density and measured tensile strength of filtered paper (Table 1). The enzymatic phosphorylation of MFC was performed to make the filtered paper more flexible and hydrophilic, indeed the introduce $-PO_4^{2-}$ groups would have positive impact on capillary adsorption of sweat which would influence the uptake of sweat from skin. In a study, a chemical approach (deep eutectic solvent based oxidation) was used for the introduction of phosphate groups and the increased flexibility of modified cellulose was reported, Furthermore, phosphorylated cellulose nanofibrils have been prepared with a maximum surface degree of substitution (DS) of 0.41 using (NH₄)₂HPO₄ in the presence of urea³².

Design and manufacturing of monitoring device

We were interested in developing highly flexible, disposable, highly accurate, and completely bio-based sensors for glucose monitoring that were adjustable based on specific variables, such as temperature, pH, and glucose concentration. As shown in Fig. 2a, an ultrathin and stretchable design that can easily be placed onto the skin and has the capability of high sweat collection *via* capillary uptake, is shown. This detachable monitoring device could easily be printed on paper (Fig. 2h). Methylated-MFC paper was fabricated using vacuum filtration (Fig. 1) and used as base for device printing (Fig. 2b). Furthermore, it demonstrated that the surface properties of paper, such as hydrophilicity/hydrophobicity, do not affect device printing. Therefore, the device was printed on hydrophilic cellulosic paper (phosphorylated-MFC paper) as shown in Fig. 2c.

Indeed, we have chosen the photolithography to create the pattern more accurate and miniature. Furthermore, we were interested to print the electrodes on cellulosic paper and due to the variability of photolithography, it could be possible for us to print electrodes on flexible paper. Furthermore, a top layer of epoxy (≈ 2 nm) was coated, the epoxy makes the whole system more stable³⁸. Furthermore, in a recent published article, three-dimensional flowerlike nickel cobalt sulfide (NiCo₂S₄) nanostructures are electrochemically deposited over the

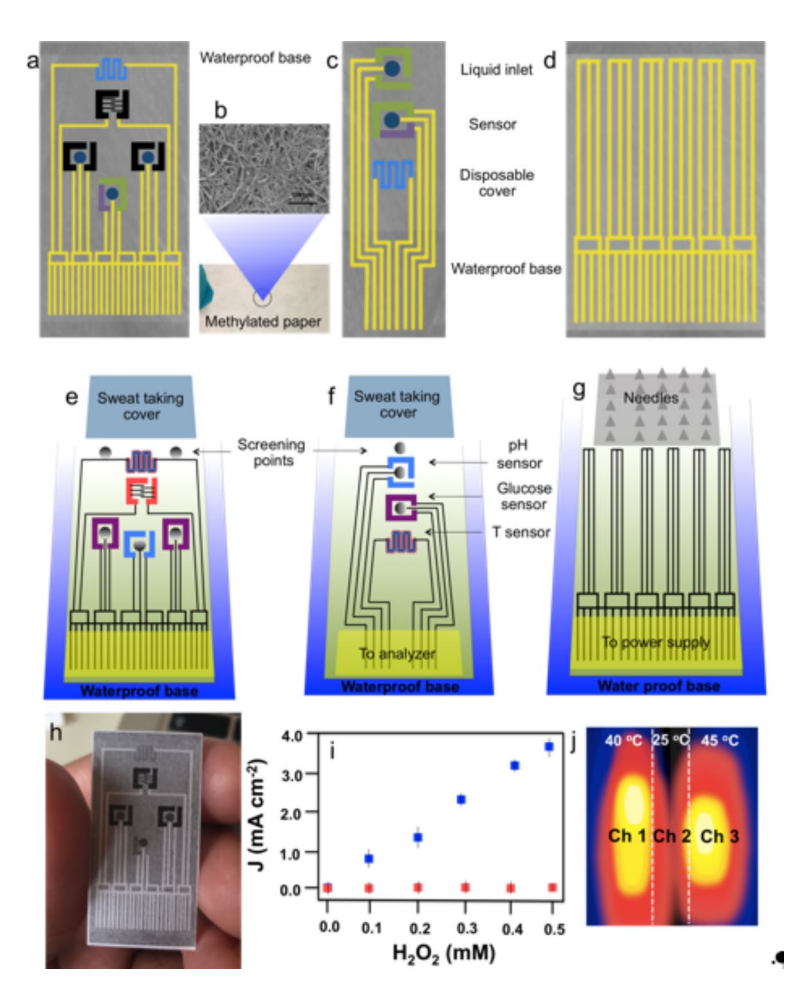


Fig. 2. Paper-based disposable glucose monitoring device and microneedles based transdermal drug delivery module. Image of fabricated sweat monitoring sensor (a) and methylated-MFC base paper captured using SEM (b). Same monitoring device has been printed on phosphorylated-MFC cellulosic paper (c) and printed power supply (d). Furthermore, systematic diagrammatic representation on device is shown in images e, f and g, images. The printed sensor is shown in image (h). A comparison of H_2O_2 sensitivity in the planer (red) and porous (blue) gold electrode deposition with Prussian blue at different H_2O_2 concentrations is shown in image (i) and infrared (IR) camera image of three-channel thermal actuator (j)

Ni-modified cellulose filter paper and the produced printed electrode was self-standing stable for monitoring of glucose from sweat³⁹. In addition, electrodeposition is also used for other metallic electrodes fabrication and no issue of falling was reported^{40–42}. Furthermore, no high level of variability of electrode fabrication and printing has been seen during batch-by-batch production and it might be due to highly smooth surface of fabricated MFC paper⁴³.

Likewise, the same system could also be used as a drug delivery device by incorporating microneedles. Microneedle-loaded drugs can easily be controlled in a multistage thermal manner (Fig. 2d). The microneedles assembled on the multichannel thermal actuator can be periodically replaced with new ones (Fig. 1). In a recent study, a colorimetric biosensor based on α -glucosidase was printed on cellulosic paper. The cellulose paper was oxidized by sodium periodate, and the C2-C3 position hydroxyl groups (–OH) on paper was oxidized to aldehyde group (–CHO), also, the amino group (–NH $_2$) of α -glu and –CHO on oxidized cellulose paper immobilized α -glu reacted through a simple Schiff base reaction to obtain Schiff-base cellulose paper. Which could screen inhibitors rapidly (in 80 s). In an another study, microneedle patch platform has been developed for the monitoring of ketone bodies, the highlight of article indicate the multi-patch system development, same as reported in the current study³². Furthermore, the study was further supported by recent published article where a paper card like sensor was developed using same reported approach and glucose was measured in tears 44 .

The whole patch-type system is schematically described in Fig. 2e-g. After applying the patch, sweat accumulates in the porous sweat-uptake layer. A waterproof band (methyl-MFC band) behind the patch aids in sweat collection and prevent delamination of the patch from the skin. A porous negatively charged Nafion membrane between the sensors and sweat uptake layer helps immobilize the GOx and remove negatively charged molecules that may affect the sensing process. A humidity sensor monitors the amount of sweat needed for reliable glucose sensing by the measuring impedance change caused by sweat generation. Above the critical sweat concentration, glucose, pH, and temperature sensors begin obtaining measurements to determine

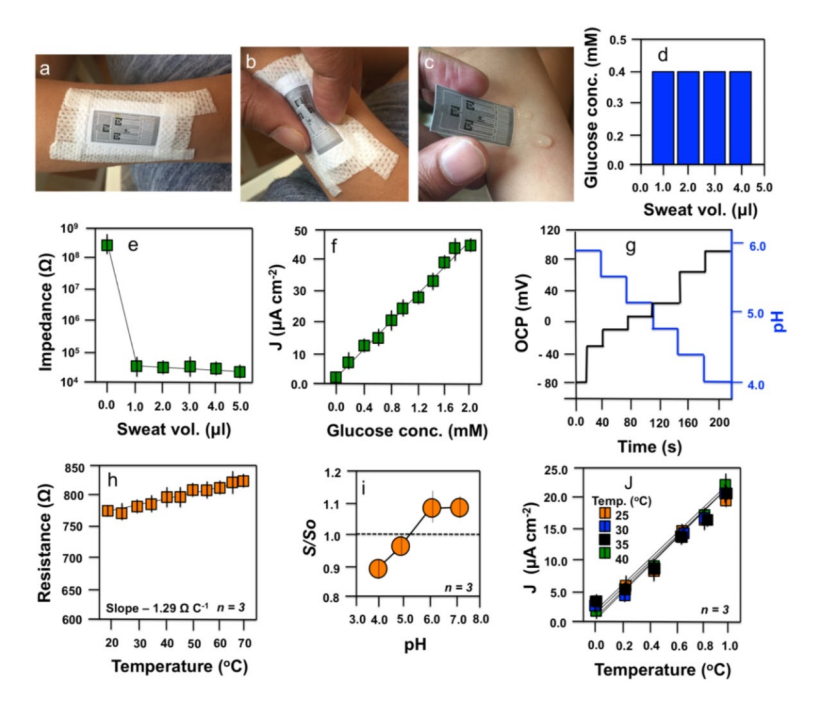


Fig. 3. Visual imaging of sensor and characterization of each sensor. The future possibility to mount the paper-based sensor on skin is shown in image (a) without delamination (b) and easily collection of sweat (c). Glucose concentration measurement at different sweat volumes is given in image (d). Calibration curves of humidity, glucose, pH and temperature are shown in images **e**, **f**, **g** and **h**, respectively. Change of the relative sensitivity of the uncorrected glucose sensor at different pH levels (i) and calibration curve of glucose sensor at different temperatures (j)

corresponding blood glucose levels. The pH and temperature sensors correct the potential errors of the enzyme-based glucose level measurement in real time. Under conditions of hyperglycemia, thermal actuation controls the feedback transdermal delivery of metformin loaded in PCNs. Same approach has been followed in a recent article, where wearable noninvasive device was provided for diverse active functionals at low \cot^{32} , four patch modular circuits based system was reported for the detection of ions in sweat. Four key sweat markers (K^+ , Ca^{2+} , Na^+ , and pH) are selected as detection targets.

Key design for monitoring glucose in sweat

A series of sensors (humidity, glucose, pH, and temperature) were designed and constructed (Fig. 2e–g) for an effective sweat-based glucose sensor. To increase detection accuracy, multipoint sensing was performed. The counter electrodes were packed as close as possible to minimize the required amount of sweat; therefore, the amount of sweat could be reduced to 1 μ l, which is a drastic decrease (20-fold) compared to a previously reported result²³. Fabrication of porous gold *via* electrodeposition facilitates an electrochemically active surface area^{45,46} and strong immobilization of enzyme (glucose oxidase)^{47,48}. To support this idea, catalysis of H_2O_2 was added to porous and planar gold electrode deposition as shown in Fig. 2i. The high level of H_2O_2 reducing catalytic activity (max 0.5 mM) of the porous network confirms the enhanced sensitivity. The cross-linked enzyme is tightly coupled to the porous network; this tight coupling also enhances the reliability of the sensor under mechanical friction and deformation.

Furthermore, the novel design of the microneedles confirms the controlled loading and delivery of drug into artificial skin. It is very clear that these microneedles can be easily replaced, and the materials used for the fabrication are biocompatible with the microneedles⁴⁹. An additional coating of phase change material (PCMs) prevents unwanted dissolution of hyaluronic acid matrix that is in contact with interstitial fluids. An SEM image of molded microneedles is given in Fig. 4c; furthermore, the heater is designed in a three-channel system (Fig. 2j) and triggers the multistage drug delivery that respond to thermal activity. It is reported in published study that low secretion rate and fast evaporation of sweat pose challenges in collection sweat from sedentary individuals for noninvasive analysis of body physiology, therefore functionalized cellulosic paper is helping to solve this problem, the high capillary force due to phosphate-MFC paper required only 1 μ l of sweat. In another approach, wearable textile combined with heating element and a microfluidic channel use to increase localized skin sweat secretion rates and combat sweat evaporation, enabling accurate and stable monitoring of trace amount of sweat³².

Optimization of sweat control

The generated sweat should be used efficiently and can be controlled by the use of methylated-MFC paper (water resistance)^{31,32} and phosphorylated-MFC paper (highly hydrophilic)³¹. The sweat uptake layer is placed on the

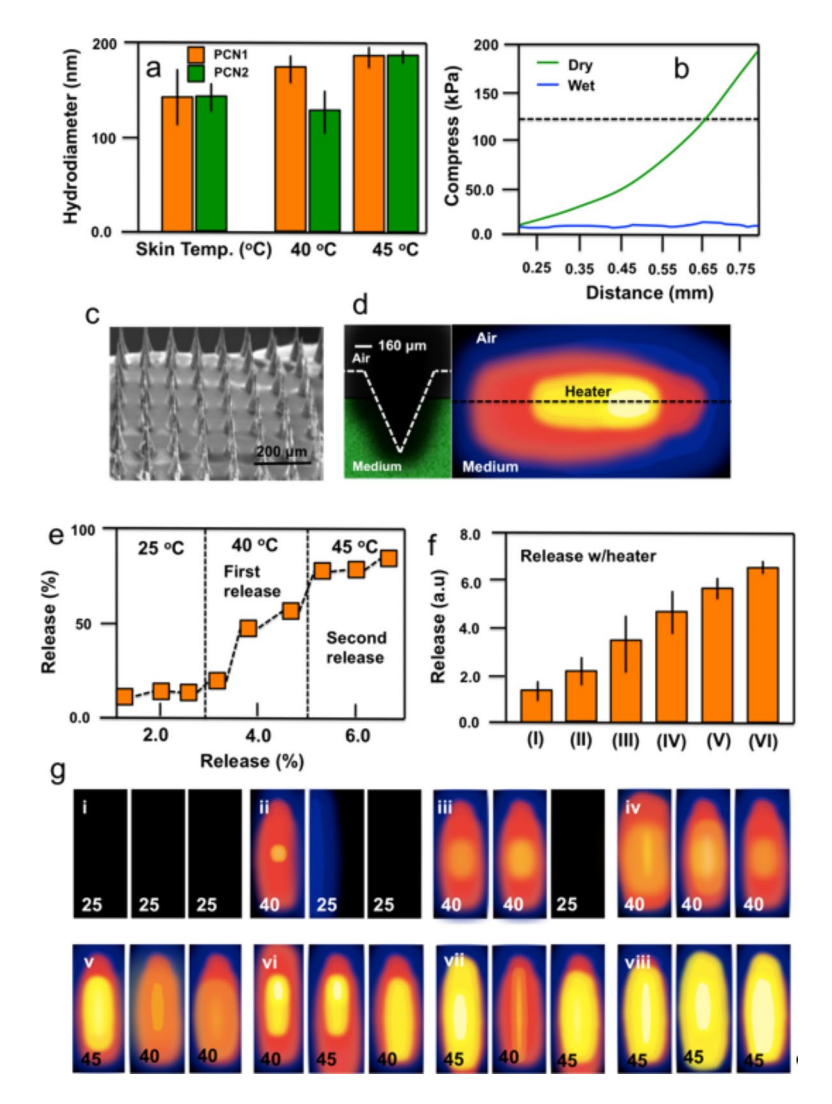


Fig. 4. Characterization of PCNs and microneedles. Dynamic light scattering size measurement of PCNs at 30 °C (skin temperature), 40 °C and 45 °C (a). Mechanical strength test of fabricated microneedles at dry and wet state (b). SEM image of produced microneedle (c). Confocal microscopy of microneedles penetrating 4% agarose gal (d, left) and IR image of the thermal actuation on the gel (d, right). Drug release profile from microneedles (e). Multistage drug-release profile (f) and IR images of eight different spatiothermal profiles using the three-channel thermal actuator for multistage drug delivery (g)

MFC papers, which absorb the sweat and then deliver it to the sensors through the Nafion membrane. The waterproof methylated-MFC paper is added on the patch cover the outside to separate the sweat from external humidity (Fig. 3a) and thus prevents delamination of the patch during skin deformation (Fig. 3b). This type of strip sensor absorbs sweat via the capillary force formed by the gap (fluidic channel), and rapid collection of sweat enables rapid sensing (Fig. 3c). The lowest concentration of glucose that we have measured without loss of sensor accuracy is 1 μ l (Fig. 3d).

Electrochemical and electrical characterization of sensors

The humidity sensor is responsible for the measurement of sweat collection via changes in impedance of the polyPEDOT in the electrode, which is the starting point of glucose measurement (Fig. 3e).

Furthermore, the glucose sensor (Prussian blue deposited porous gold electrode) is calibrated using a galvanostatic method (Fig. 3f). The glucose concentrations (10 μ M and 1 mM) are in the ranges of both hypoglycemic and hyperglycemic patients and healthy subjects^{26,27}. The glucose sensor was stable under mechanical deformation (Supplementary file, Figure S2), indicate no deformation, and selectively detected glucose over other biomolecules (including ascorbic, uric, and lactic acids)^{50,51} and drugs, including acetaminophen, acetylsalicylic acid, and metformin (Supplementary file, Figure S3)^{52,53}.

The enzyme-based glucose sensor fluctuates at different pH values (Supplementary file, Figure S4). Thus, the pH sensor was calibrated using standard pH buffer solutions (Fig. 3g, Supplementary file, Figure S5) and maintains stable operation under deformation (Supplementary file, Figure S6). Furthermore, the resistor-based temperature sensor for skin temperature monitoring was also calibrated (Fig. 3h). The concurrent use of these

co-integrated sensors can enhance the accuracy of glucose sensing. For example, the metabolic secretion of lactic acid in sweat causes the pH level to decrease to 4 or 5. The concurrent pH sensing along with glucose sensing can correct this pH-dependent deviation (Fig. 3i) of the enzyme-based glucose sensor; furthermore, the pH sensor in the current setting does not show the significant fluctuation at different temperatures (Fig. 3j).

Different temperature-dependent stepwise drug delivery systems were developed. The used palm oil (PCN1, $T_m=38\,^{\circ}\mathrm{C}$) and tridecanoic acid PCN2, ($T_m=43\,^{\circ}\mathrm{C}$), which melt below the temperature of the skin (30 °C). Metformin was embedded in the PCM matrix. The novel phase transfer of the PCM was temperature-dependent (solid at lower T and liquid at higher T), Furthermore, cytotoxicity testing showed that the system was nontoxic and biocompatible and thus suitable for medical applications. Hydrodynamic diameters (Fig. 4a) of PCNs fluctuated with respect to temperature. In this study, the "switch system" in which a temperature increase is reflected as a change in skin temperature (30 °C) to above melting temperatures (40 or 45 °C), and the PCM matrices can block drug release before such thermal changes occur. Furthermore, when the temperature reached 40 °C, only the drugs contained in PCN1 were released, whereas at 45 °C, drugs in both PCN1 and 2 were released (Fig. 4a).

This, multilayer-patch is new design that could measure the glucose level in sweat, in a recent study, same design of electrochemical sensor was used, the author called it sandwich model of sensing, where the Prussian blue nanoparticles and carboxylated carbon nanotubes were self-assembled on the electrode to improve the electrochemical performance and as the sensor unit, glucose oxidase was immobilized by chitosan as the reactions catalysis unit and finally encapsulated with Nafion to ensure a stable performance. The results indicate a low detection limit (7.0 μ M) of glucose in sweat, high sensitivity (11.87 μ A mM⁻¹ cm⁻²), and excellent resistance for a full sweat glucose application range (0.0–1.0 mM)⁵³. Luckily, current functionalized cellulosic sensor multilayer-patch system is more sensitive, accurate and flexible compared to reported literature. Recently, a very fine review has been published about the wearable devices for the glucose monitoring, which indicate the emerging trends for development of noninvasive devices for the monitoring of glucose in biomarkers. The review further demonstrates the high number of publications in the filed on multilayer patch system sensing design and development⁵³.

Microneedles fabrication and drug delivery

The microneedles were fabricated using molding as reported in the methods section. The microneedles were stiff enough to penetrate the agarose gel (Fig. 4b). The SEM image of the fabricated microneedles is given in Fig. 4c and confirms penetration of the formed agarose gel (corresponding to skin in this article) by the pointed end⁵⁴. The produced microneedles could penetrate a 4% agarose gel and could generate pores (Fig. 4d, left) after penetration by microneedles. Vertical heat transfer dissolved the outside PCM coating and embedded PCNs. The vertical temperature distribution of the agarose gel imaged with an infrared (IR) camera confirmed the successful heat transfer (Fig. 4d, right).

To investigate the stepwise drug release into agarose gel, we heated the microneedles containing dyes from 25 to 45 $^{\circ}\mathrm{C}$ (Fig. 4e). An insignificant release of drug was analyzed around the skin temperature (30 $^{\circ}\mathrm{C}$) due to availability of PCNs, but at the elevated temperature (40 $^{\circ}\mathrm{C}$), the PCM coating and PCN1 dissolved, and the metformin in PCN1 was released. At the higher temperature (45 $^{\circ}\mathrm{C}$), metformin in both PCN1 and 2 was released. The six-stage programmed dye release profile (Fig. 4f) and heater consisting of the three channels together with two types of PCNs resulted in eight different spatiothermal patterns as shown in Fig. 4g.

Glucose monitoring in sweat

Paper based disposable sensors are used for monitoring of glucose in sweat for which the paper sensor is connected to skin (Fig. 5a). The monitoring starts with humidity sensing to determine the optimal point to start sweat analysis (Fig. 5b). When the sweat-uptake layer absorbs enough sweat, the glucose and pH sensors detect the glucose concentration and pH level in the sweat, respectively. We explained that triple and quadruple pH sensing improved the detection accuracy (Fig. 5c). The correction using the measured pH enabled more accurate glucose sensing (Fig. 5d).

The disposable strip-type sensor is more convenient for the sweat analysis. The strip-type sensor first absorbed sweat because of capillary flow. The absorbed sweat should cover the surface of both the pH and glucose sensors. The amount of absorbed sweat could be monitored by measuring the impedance between the electrode of the glucose and pH sensors (Fig. 5e). The strip-type sensor could be stably operated using 4 μ l of sweat. After the sweat covers both the glucose and pH sensors, the measurements begin (Fig. 5f).

The pH levels in the sweat vary among subjects. Depending on the physiological conditions of each subject, the sweat glucose levels corrected by pH measurements before and after a meal (Fig. 5g) agree well with the sweat glucose levels measured among subjects using a commercial glucose kit assay (Fig. 5h). The resulting data were so accurate and indicated that blood glucose concentrations tend to vary before and after a meal, like the measured sweat glucose concentrations (Fig. 5i).

Microneedle-based controlled drug delivery

Artificial transdermal drug delivery was conducted on agarose gel artificial skin having diabetic artificial solution. A control without a patch (black, Fig. 5i), microneedles without diabetes drug (red, Fig. 5i), and microneedles with diabetes drugs (blue with one dose and green with another dose, Fig. 5i) were used. The sweat glucose data correlated well with obtained glucose levels beneath the artificial skin. For precise and timely drug delivery, two types of metformin-loaded PCNs were embedded in the PCM-coated microneedles. The thermoresponsive microneedles controlled by multichannel heaters enabled the multistage and spatially patterned artificial transdermal drug release in response to the measured sweat glucose levels. Furthermore, the literature also reveals the array of microneedle sensing device which work for real time monitoring in human

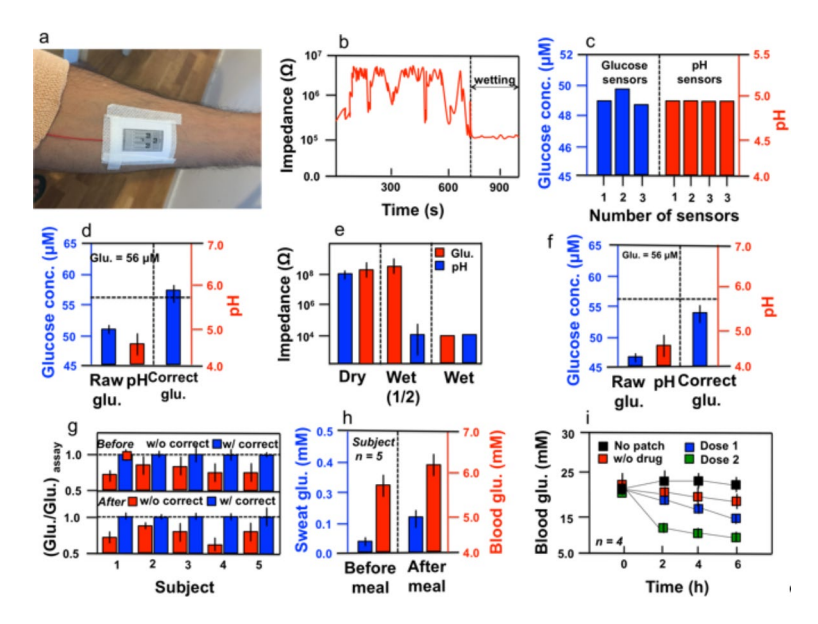


Fig. 5. Sweat based glucose monitoring. The image shows the future utilization of produced device during exercise (**a**). Real-time humidity monitoring to check the accumulation of sweat (**b**). Multimodal glucose and pH sensing to improve detection accuracy (**c**). Measured sweat glucose concentrations (n = 3), pH levels (n = 4), (**d**) and corrected sweat glucose level (n = 3) based on the averaged pH (dotted line, glucose concentration measured by a commercial glucose assay) (**e**). Sweat glucose and pH monitoring using the disposable strip (**f**). Humidity monitoring of the disposable strip using impedance measurements. **g** Sweat glucose and pH monitoring using the disposable strip (**h**). Ratio of sweat glucose concentrations (n = 3) measured by the patch and a commercial glucose assay with and without the pH-based correction before and after a meal (**i**)

interstitial fluids (lower conc. of glucose compared to blood), same approach (as reported in current study) was followed, reported sensors are integrated in a single sensing patch, thus electrodes could eliminate common-mode interference signals, thus significantly improving the detection accuracy⁵³. By optimizing the structure of the microneedle, the puncture efficiency was improved while the puncture force was reduced.

Conclusion

We report a novel material structure, device design, and system integration strategy for a sweat glucosemonitoring device integrated with feedback transdermal drug delivery microneedles. For efficient sweat control and sensing, the sweat monitoring patch was assembled with multiple sweat-uptake and waterproof methylated-MFC layers, and sensor sizes were miniaturized to the point that $\sim 1~\mu l$ of sweat was sufficient for obtaining a reliable measurement. The measurements of sweat glucose levels with real-time corrections based on pH, temperature, and humidity sensing were found to be accurate under various environmental changes. The sweat glucose data correlated well with blood glucose levels. For precise and timely drug delivery, two types of metformin-loaded PCNs were embedded in the PCM-coated microneedles. The thermoresponsive microneedles controlled by multichannel heaters enable the multistage and spatially patterned transdermal drug release in response to the measured sweat glucose level.

For practical application of the current system, several things should be improved. Long-term stability and uniformity of sensors are particularly important for making the system practical and applicable to human subjects without the need for multiple recalibrations. Further, another kind of drug (for example, chlorpropamide) can be loaded for synergistic treatment or fast regulation of blood glucose levels. With further improvements in these points, clinical translation can be pursued for sweat-based sensing and feedback therapy. The current system provides important new advances toward the painless and stress-free point-of-care treatment of diabetes mellitus.

Data availability

Data is available on the request to corresponding author.

Received: 21 August 2024; Accepted: 30 September 2024 Published online: 08 October 2024

References

 Wu, J., Liu, Y., Yin, H. & Guo, M. A new generation of sensors for non-invasive blood glucose monitoring. Am. J. Translational Res. 15, 3825 (2023).

- Badugu, R., Lakowicz, J. R. & Geddes, C. D. A glucose-sensing contact lens: from bench top to patient. Curr. Opin. Biotechnol. 16, 100–107 (2005).
- 3. Makaram, P., Owens, D. & Aceros, J. Trends in nanomaterial-based non-invasive diabetes sensing technologies. *Diagnostics.* 4, 27–46 (2014).
- Mitsubayashi, K. & Arakawa, T. Cavitas sensors: contact lens type sensors & mouthguard sensors. Electroanalysis. 28, 1170–1187 (2016).
- 5. Witkowska Nery, E., Kundys, M., Jelen, P. S. & Jönsson-Niedziółka, M. (ACS, (2016).
- 6. WHO. Report of the WHO discussion group for people living with diabetes: virtual meeting. 23. (2023).
- 7. Cha, K. H., Jensen, G. C., Balijepalli, A. S., Cohan, B. E. & Meyerhoff, M. E. Evaluation of commercial glucometer test strips for potential measurement of glucose in tears. *Anal. Chem.* 86, 1902–1908 (2014).
- 8. Wong, N. D. & Sattar, N. Cardiovascular risk in diabetes mellitus: epidemiology, assessment and prevention. *Nat. Reviews Cardiol.* **20**, 685–695 (2023).
- 9. Coles, B. et al. Cardiovascular events and mortality in people with and without type 2 diabetes: an observational study in a contemporary multi-ethnic population. *J. Diabetes Invest.* 12, 1175–1182 (2021).
- 10. Wang, J. Electrochemical glucose biosensors. Chem. Rev. 108, 814-825 (2008).
- 11. Pappa, A. M. et al. Organic electronics for point-of-care metabolite monitoring. Trends Biotechnol. 36, 45-59 (2018).
- 12. Kim, J., Campbell, A. S. & Wang, J. Wearable non-invasive epidermal glucose sensors: a review. Talanta. 177, 163-170 (2018).
- 13. Wang, J. Carbon-Nanotube based electrochemical biosensors: a review. Electroanalysis: Int. J. Devoted Fundamental Practical Aspects Electroanalysis. 17, 7–14 (2005).
- 14. Grieshaber, D., MacKenzie, R., Vörös, J. & Reimhult, E. Electrochemical biosensors-sensor principles and architectures. *Sensors.* 8, 1400–1458 (2008).
- 15. Panwar, S. et al. Portable optical biosensor for point-of-care monitoring of salivary glucose using a paper-based microfluidic strip. *Biosens. Bioelectronics: X.* 17, 100452 (2024).
- 16. Giaretta, J. et al. Glucose sensing in saliva. Adv. Sens. Res. 2400065 (2024).
- 17. Chen, Y. et al. A wearable non-enzymatic sensor for continuous monitoring of glucose in human sweat. *Talanta.* **278**, 126499 (2024).
- Wei, X. et al. Wearable biosensor for sensitive detection of uric acid in artificial sweat enabled by a fiber structured sensing interface. Nano Energy. 85, 106031 (2021).
- 19. Ma, S., Yuan, X., Yin, X., Yang, Y. & Ren, L. A silver nanowire aerogel for non-enzymatic glucose detection. *Microchem. J.* 195, 109324 (2023).
- 20. Bandodkar, A. J. et al. Tattoo-based noninvasive glucose monitoring: a proof-of-concept study. Anal. Chem. 87, 394-398 (2015).
- 21. Gao, W. et al. Wearable microsensor array for multiplexed heavy metal monitoring of body fluids. Acs Sens. 1, 866-874 (2016).
- 22. Gao, W. et al. Fully integrated wearable sensor arrays for multiplexed in situ perspiration analysis. Nature. 529, 509-514 (2016).
- 23. Lee, H. et al. A graphene-based electrochemical device with thermoresponsive microneedles for diabetes monitoring and therapy. *Nat. Nanotechnol.* 11, 566–572. https://doi.org/10.1038/nnano.2016.38 (2016).
- Imani, S. et al. A wearable chemical–electrophysiological hybrid biosensing system for real-time health and fitness monitoring. Nat. Commun. 7, 11650 (2016).
- 25. Kim, J. et al. Noninvasive alcohol monitoring using a wearable tattoo-based iontophoretic-biosensing system. Acs Sens. 1, 1011–1019 (2016).
- 26. Moyer, J., Wilson, D., Finkelshtein, I., Wong, B. & Potts, R. Correlation between sweat glucose and blood glucose in subjects with diabetes. *Diabetes. Technol. Ther.* 14, 398–402 (2012).
- 27. Sakaguchi, K. et al. Evaluation of a minimally invasive system for measuring glucose area under the curve during oral glucose tolerance tests: usefulness of sweat monitoring for precise measurement. J. Diabetes Sci. Technol. 7, 678–688 (2013).
- 28. Karim, Z., Georgouvelas, D., Svedberg, A., Monti, Ś. & Mathew, A. P. Upscaled engineered functional microfibrillated cellulose flat sheet membranes for removing charged water pollutants. Sep. Purif. Technol. 289, 120745 (2022).
- 29. Group, U. P. D. S. Effect of intensive blood-glucose control with metformin on complications in overweight patients with type 2 diabetes (UKPDS 34). *Lancet.* **352**, 854–865 (1998).
- 30. Prausnitz, M. R. & Langer, R. Transdermal drug delivery. Nat. Biotechnol. 26, 1261–1268 (2008).
- 31. Karim, Z. & Monti, S. Microscopic hybrid membranes made of cellulose-based materials tuned for removing metal ions from industrial effluents. ACS Appl. Polym. Mater. 3, 3733–3746 (2021).
- 32. Karim, Z. et al. Enhanced sieving of cellulosic microfiber membranes via tuning of interlayer spacing. *Environ. Science: Nano.* 7, 2941–2952 (2020).
- 33. Karim, Z., Svedberg, A. & Ayub, S. Role of functional groups in the production of self-assembled microfibrillated cellulose hybrid frameworks and influence on separation mechanisms of dye from aqueous medium. *Int. J. Biol. Macromol.* **155**, 1541–1552 (2020).
- 34. Ogeda, T. L., Silva, I. B., Fidale, L. C., Seoud, E., Petri, D. F. & O. A. & Effect of cellulose physical characteristics, especially the water sorption value, on the efficiency of its hydrolysis catalyzed by free or immobilized cellulase. *J. Biotechnol.* 157, 246–252 (2012).
- 35. Chen, C. L. in In Methods in Lignin Chemistry. 301-321 (eds Lin, S. Y., Carlton, W. & Dence) (Springer, 1992).
- 36. Viera, R. G. et al. Synthesis and characterization of methylcellulose from sugar cane bagasse cellulose. *Carbohydr. Polym.* 67, 182–189 (2007).
- 37. Karim, Z., Khan, M. J., Hussain, A., Ahmed, F. & Khan, Z. H. Impact of functionalized and structurally tuned cellulosic composite membranes on removal of metal ions, dye, drug, and proteins. *Colloids Surf.*, a. 692, 134031 (2024).
- 38. Ansari, F., Lindh, E. L., Furo, I., Johansson, M. K. G. & Berglund, L. A. Interface tailoring through covalent hydroxyl-epoxy bonds improves hygromechanical stability in nanocellulose materials. *Compos. Sci. Technol.* 134, 175–183. https://doi.org/10.1016/j.compscitech.2016.08.002 (2016).
- 39. Babu, K. J., Kumar, R., Yoo, T. & Phang, D. J. Gnana Kumar, G. Electrodeposited nickel cobalt sulfide flowerlike architectures on disposable cellulose filter paper for enzyme-free glucose sensor applications. ACS Sustain. Chem. Eng. 6, 16982–16989 (2018).
- Guo, Y. et al. Batch fabrication of H2S sensors based on evaporated Pd/WO3 film with ppb-level detection limit. Mater. Chem. Phys. 302, 127768 (2023).
- 41. Min, J. et al. Recent advances in biodegradable green electronic materials and sensor applications. Adv. Mater. 35, 2211273 (2023).
- 42. Sung, D. H. et al. Scalable, roll-to-roll manufacturing of multiscale nanoparticle/fiber composites using electrophoretic deposition: novel multifunctional in situ sensing applications. *Compos. Sci. Technol.* 245, 110322 (2024).
- 43. Hobbie, H. A., Doherty, J. L., Smith, B. N., Maccarini, P. & Franklin, A. D. Conformal printed electronics on flexible substrates and inflatable catheters using lathe-based aerosol jet printing. *npj Flex. Electron.* **8**, 54 (2024).
- 44. Fiore, L. et al. Paper card-like electrochemical platform as a smart point-of-care device for reagent-free glucose measurement in tears. *Chem. Commun.* **59**, 4300–4303 (2023).
- 45. Niu, Z. et al. A universal strategy to prepare functional porous graphene hybrid architectures. Adv. Mater. 26, 3681–3687 (2014).
- 46. Wang, W. et al. Bioinspired Nanosucker array for enhancing Bioelectricity Generation in Microbial Fuel cells. *Adv. Mater. (Deerfield Beach Fla)*. **28**, 270–275 (2015).
- Pan, L. et al. Hierarchical nanostructured conducting polymer hydrogel with high electrochemical activity. Proc. Natl. Acad. Sci. 109, 9287–9292 (2012).
- 48. Claussen, J. C. et al. Nanostructuring platinum nanoparticles on multilayered graphene petal nanosheets for electrochemical biosensing. *Adv. Funct. Mater.* **22**, 3399–3405 (2012).

- Singh, A. et al. Enhanced lubrication on tissue and biomaterial surfaces through peptide-mediated binding of hyaluronic acid. Nat. Mater. 13, 988–995 (2014).
- 50. Wenzhao, J., Xuan, W., Julian, R. & Joseph, W. Tattoo-based noninvasive glucose monitoring: a proof-of-concept study. (2015).
- 51. Harvey, C. J., LeBouf, R. F. & Stefaniak, A. B. Formulation and stability of a novel artificial human sweat under conditions of storage and use. *Toxicol. In Vitro.* 24, 1790–1796 (2010).
- 52. Tang, Z., Du, X., Louie, R. F. & Kost, G. J. Effects of drugs on glucose measurements with handheld glucose meters and a portable glucose analyzer. *Am. J. Clin. Pathol.* 113, 75–86 (2000).
- Hirst, J. A., Farmer, A. J., Ali, R., Roberts, N. W. & Stevens, R. J. Quantifying the effect of metformin treatment and dose on glycemic control. *Diabetes care*. 35, 446–454 (2012).
- 54. Prausnitz, M. R. Microneedles for transdermal drug delivery. Adv. Drug Deliv. Rev. 56, 581-587 (2004).

Acknowledgements

The authors thank the generous support from the researchers supporting project number (RSPD2024R980), King Saud University, Riyad, Saudi Arabia.

Author contributions

ZK= Editing final manuscript, Idea, Supervision and Methodology. MJK= Experimental setup, Formal analysis and Investigation. AH= Funding and Supervision. FH= Supervision, Materials, and editing of draft. ZHK= Supervision, Editing of draft manuscript, methodology.

Declarations

Competing interests

The authors declare no competing interests.

Additional information

Supplementary Information The online version contains supplementary material available at https://doi.org/10.1038/s41598-024-74899-z.

Correspondence and requests for materials should be addressed to Z.K.

Reprints and permissions information is available at www.nature.com/reprints.

Publisher's note Springer Nature remains neutral with regard to jurisdictional claims in published maps and institutional affiliations.

Open Access This article is licensed under a Creative Commons Attribution-NonCommercial-NoDerivatives 4.0 International License, which permits any non-commercial use, sharing, distribution and reproduction in any medium or format, as long as you give appropriate credit to the original author(s) and the source, provide a link to the Creative Commons licence, and indicate if you modified the licensed material. You do not have permission under this licence to share adapted material derived from this article or parts of it. The images or other third party material in this article are included in the article's Creative Commons licence, unless indicated otherwise in a credit line to the material. If material is not included in the article's Creative Commons licence and your intended use is not permitted by statutory regulation or exceeds the permitted use, you will need to obtain permission directly from the copyright holder. To view a copy of this licence, visit http://creativecommons.org/licenses/by-nc-nd/4.0/.

© The Author(s) 2024